ELSEVIER

Journal of Power Sources 86 (2000) 309–315

JOURNAL OF POWER SOURCES

www.elsevier.com/locate/jpowsour

Analysis by electrochemical impedance spectroscopy of new MCFC cathode materials

F.J. Pérez [a], D. Duday [a,*], M.P. Hierro [a], C. Gómez [a], M. Romero [a], M.T. Casais [b], J.A. Alonso [b], M.J. Martínez [b], L. Daza [c]

[a] *Universidad Complutense de Madrid, Facultad de Ciencias Químicas, Departamento de Ciencia de los Materiales, 28040 Madrid, Spain*
[b] *Instituto de Ciencia de Materiales (CSIC), Campus UAM-Cantoblanco, 28049 Madrid, Spain*
[c] *Instituto de Catálisis y Petroleoquímica (CSIC)-CIEMAT, Campus UAM-Cantoblanco, 28049 Madrid, Spain*

Accepted 13 October 1999

Abstract

The corrosion and electrochemical behaviours of $Li_{1-x}Ni_{1+x}O_2$ and $Li_{1-x}(Ni_yCo_{1-y})_{1+x}O_2$ oxides were investigated in a molten carbonate electrolyte at 650°C and compared with a NiO reference cathode material. These oxides are future candidate cathode materials for molten carbonate fuel cell (MCFC) and are divided in two families: monophasic oxides and biphasic oxides. The monophasic oxides show an important dissolution or a lower catalytic activity and are not good candidates for future use in MCFC. The biphasic oxides show a low dissolution and a good catalytic efficiency close to the NiO value. In this first study of new cathode materials by electrochemical impedance spectroscopy (EIS), it appears that the biphasic Li–Ni–Co–O oxides are the best candidates for MCFC. The MCFC electrochemical cathodic mechanism, taking into account the peroxide and the superoxide pathways and the O_2^-, CO_2 and H_2O diffusion proposed in the bibliography [I. Uchida, T. Nishina, Y. Mugikura, K. Itaya, J. Electroanal. Chem., 206 (1986) 229; C. Yuh, J.R. Selman, AIChE J., 34(12) (1988) 1949; T. Nishina, I. Uchida, Proc. Symp. Molten Carbonate Fuel Cell Technol., The Electrochem. Soc., PV90-16 (1990) 438; T. Nishina, G. Lindbergh, T. Kudo, I. Uchida, The International Fuel Cell Conference Proceedings, NEDO (1992) 189–192], is used to discuss the EIS results. The limiting rate of the peroxide or/and superoxide reactions of the new oxides was compared with the NiO reference oxide.

Keywords: Li–Ni–Co–O oxides; Molten carbonate; Fuel cell; Cathode; Reduction mechanism

1. Introduction

In molten carbonate fuel cell (MCFC) technology, the dissolution of the NiO cathode in molten carbonate and the degradation of the $LiAlO_2$ matrix are the major lifetime limiting factors [1]. To overcome the problem of cathode dissolution, new cathode materials have to be developed. In this work, four new Li–Ni–(Co)–O oxides have been studied by the electrochemical impedance spectroscopy (EIS) technique and long term in-situ electrochemical measurements were carried out for the first time in molten carbonate.

Two different aspects of the study of MCFC cathodes are reviewed here in order to fully understand the aims of this work. The first aspect concerns the use of the ac impedance technique to determine the oxygen reduction mechanism at the cathode–molten carbonate interface. In the second part, the structure and the composition of the cathode materials and their effects on the dissolution in molten carbonate are described.

In the MCFC cathodes studies, the EIS technique was generally used to determine the electrochemical mechanisms which occur with smooth or porous oxide cathodes in contact with molten carbonate and the MCFC gas atmosphere.

It has been shown by EIS that the oxygen reduction mechanism is limited by the peroxide or superoxide ions reduction or by the CO_2, O_2^- and molecular oxygen diffusions [2–7] depending of the experimental parameters.

It is thought that the oxygen reduction mechanism does not change with the cathode material but is very dependent on the gas composition and the rate of coverage of the oxide ions on the cathode surface [7,8].

* Corresponding author. Tel.: +34-91-394-4215; fax: +34-91-394-4357; e-mail: dduday@eucmos.sim.ucm.es

0378-7753/00/$ - see front matter
PII: S0378-7753(99)00422-X

The influence of water on the oxygen reduction mechanism in MCFC has also been studied by EIS and it was shown that water does not change the reduction mechanism but it can modify the apparent oxygen reduction rate in a CO_2 diffusion limiting case [9,10].

Freni et al. [11] have reviewed the NiO cathode mechanism, development and limits as MCFC cathodes. Li^+ ions, coming from the electrolyte, diffuse into the NiO oxide and significantly increase its electronic conductivity. During the in-situ oxidation and lithiation processes, a modification of the cathode structure occurs: pores of a smaller diameter than 1 μm appear between the initially largest pores (7 to 15 μm) of the NiO layer. This porosity eases the reduction reactions which take place in a three-phase (solid–liquid–gas) mechanism occurring at the MCFC cathode surface and give the NiO oxide good properties as MCFC cathode. However, the NiO dissolution in the melt limits the lifetime of the cell and despite the improvement of the NiO cathode [12], other materials need to be developed.

$LiFeO_2$ and $LiCoO_2$ were investigated as NiO alternative materials [7,13–16]. These oxides show a good behaviour particularly in the case of $LiCoO_2$, but at the working pressure ($P = 5$ atm), the solubility of this oxide tends to the NiO value [16].

Recently, a new generation of oxide which contain a second metal element and/or a high lithium content have been proposed in order to obtain higher melt resistant and conducting cathode materials. The modified-NiO oxides represent the most recent alternatives to the NiO cathodes. Yang and Kim [17] have compared the molten carbonates solubility of lithiated NiO and lithiated (Ni,Co)O formed by in-situ oxidation and lithiation of Ni and Ni–Co alloy porous plaques under cathodic MCFC conditions. They showed that the Co-containing oxide solubility is much lower than NiO and that the solubility decreased with Co content increase. An addition of Co to the Ni-based cathode material has been shown to be a method to lower the solubility of the NiO cathodes in molten carbonates [17].

Recent work showed that $Li_xNi_{1-x}O$ with high lithium content ($x < 0.2$) has a relatively lower rate of dissolution than $Li_xNi_{1-x}O$ with low lithium content ($0.02 < x < 0.05$) obtained with the in-situ oxidized and lithiated NiO [18]. Hatoh et al. have also shown that the change of lithium concentration in the high-lithium-content-cathode is very small after immersion of the cathode in the melt unlike that the low-lithium-content-cathode.

Other researchers have proposed high-lithium-content-cathodes and shown a relationship between the lithium content and the porosity of the cathode. The porosity increased with the Li content up to 23 at.% Li and then this porosity was nearly constant for higher contents [19].

Baranda [20] and Daza [21] studied the effect of additions of rare earth elements on the behaviour of NiO cathodes in molten carbonate by the powder metallurgy technology. They showed that an addition of less than 1.0% of rare earth elements allows a decrease of the dissolution rate, with an increase of the lithiation rate and of the electronic conductivity of the NiO cathode. In this work, for $Li_xNi_{1-x}O$ oxides, it was shown that an x-value of 0.33 is optimal to obtain a lower dissolution rate of the cathode in molten carbonate and a higher electronic conductivity.

The original aim of our study has been to continue the work developed by Yang and Kim [17] and by Daza [21] to formulate new oxides. Moreover, these new oxides were tested by ac-impedance for long testing times in molten carbonate. This work is the first to propose a determination of the dissolution rate of the oxide and of the O_2 reduction mechanism at the cathode surface using the ac-impedance technique in combination with X-Ray Diffraction (XRD) and Scanning Electron Microscopy (SEM).

2. Experimental

Electrochemical tests were performed at 650°C in an alumina crucible. We used an atmosphere of gases formed during the melting process.

The working electrode is composed of the sample studied connected to a wire lead that is shielded from the electrolyte by an alumina tube and a ceramic seal-place at the base of the tube. The reference/counter electrode is identical to the working electrode. This system with two electrodes is easier to apply in these difficult conditions because a complex reference electrode cannot operate for long times. The carbonate mixture used as electrolyte was the eutectic mixture of lithium and potassium carbonate (62 mol% Li_2CO_3 and 38 mol% K_2CO_3). The materials tested were $Li_{1-x}Ni_{1+x}O_2$ and $Li_{1-x}(Ni_yCo_{1-y})_{1+x}O_2$ oxides with x between 0 and 0.5 and $y > 0.5$ (y is constant); they were prepared by powder metallurgy and sol–gel techniques [20,21]. The oxide-1 and oxide-2 only differ in the Li content which is lower in the oxide-2. The preparation of oxide-3 and oxide-4 is identical to oxide-1 and oxide-2 except it includes the addition of Co. The oxide-3 and oxide-4 only differ in their Li content that is lower in the oxide-4. The Li/(Co, Ni) ratio is identical for oxide-1 and oxide-3 and for oxide-2 and oxide-4 for

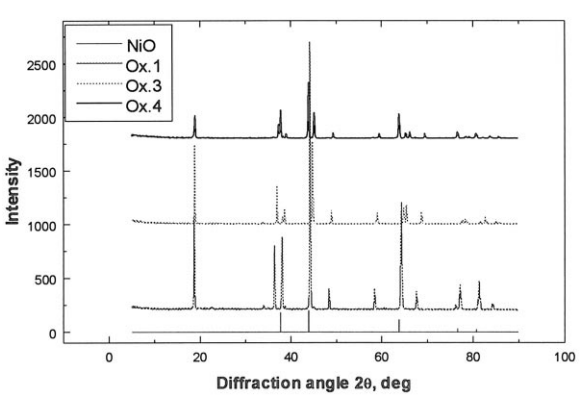

Fig. 1. Superimposed XRD spectra of the oxides before immersion.

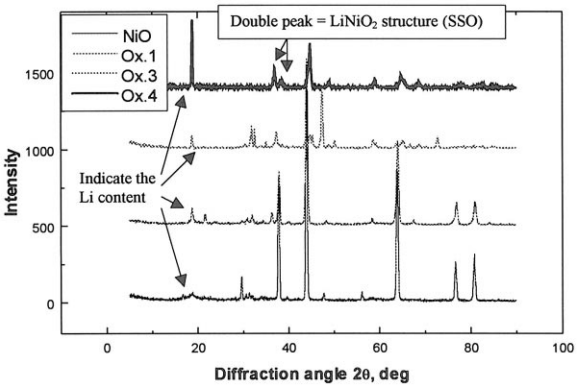

Fig. 2. Superimposed XRD spectra of the oxides after immersion in a 62/38 mol% Li_2CO_3/K_2CO_3 eutectic mixture at 650°C under air. Time of immersion: 4 days for oxide-3 and 7 days for the others.

another part. A NiO cathode was used as reference. The specimens ($6 \times 15 \times 2$ mm^3) were attached to a 0.5-mm wire of chromel. The EIS measurements were started 2 h after immersion in the melt in order to obtain a sufficiently stabilized system necessary for an ac-impedance experiment. Various measurements were made from 2 to 200 h. The EIS characterization was generally carried out for shorter times than the XRD and SEM characterizations because of the degradation of the electrode materials during the experiment. A 5-mV perturbation amplitude was applied with a frequency scanning range of 10 mHz to 30 kHz. All experiments were recorded with a frequency response analyzer Solartron 1255 and a potentiostat EG&G 283.

After each experiment, the corroded specimens were taken out of the melt, rinsed with distilled water and investigated by XRD and SEM.

3. Results

3.1. Microstructural characterization

3.1.1. XRD characterization

In Figs. 1 and 2, it can be seen that none of the oxides tested retained the same structure after 1 week of immersion in molten carbonate at 650°C, but two of them still presented a mixed oxide structure at the end of the test; the NiO oxide exhibited a quasi-$LiNiO_2$ structure and the $Li_{1-x}(Ni_yCo_{1-y})_{1+x}O_2$ oxide with $0.5 > x > 0.2$ exhibited a mainly $LiCoO_2$ structure. The oxides with a high content of lithium seem to decompose into the base oxide (NiO, Co_3O_4) and other Li products and, the Ni oxides with a lower Li-content show a low stability in molten carbonate. The $Li_{1-x}Co_{1+x}O_2$ phases with a lower x value ($0.5 > x > 0.2$) showed the best behaviour.

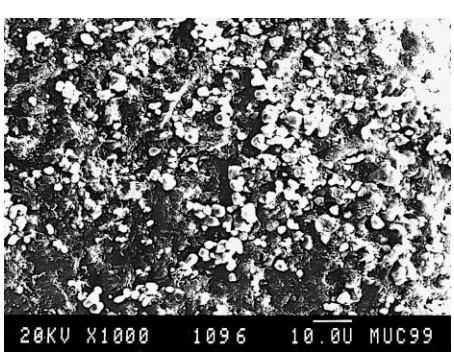

Fig. 3. SEM micrograph of a corroded surface of oxide-3 after 4 days exposure time. The surface is degraded.

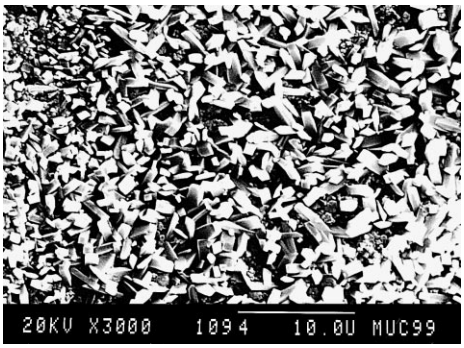

Fig. 4. SEM micrograph of a corroded surface of oxide-4 after 7 days exposure time. The surface shows a homogeneous crystalline structure.

3.1.2. SEM characterization

After 4 days immersion in molten salt, the $Li_{1-x}(Ni_yCo_{1-y})_{1+x}O_2$ oxide with $x < 0.2$ (oxide-3) is considerably degraded with an external zone composed of few equiaxial grains located on a dense phase (Fig. 3) and an inner zone with only equiaxial grains. The electrolyte penetration is deeper than 200 μm. The dense phase shows decomposition of the initial oxide into an amorphous compound as detected by XRD (Fig. 2). In conclusion, the oxide 3 is characterized by a low degree sintering and a significant degradation in molten carbonate after 4 days of immersion.

The $Li_{1-x}(Ni_yCo_{1-y})_{1+x}O_2$ oxide with $0.5 > x > 0.2$ (oxide-4) shows two different zones after an immersion of 7 days in molten carbonate. The external zone is composed of very small equiaxial grains and the internal zone of very

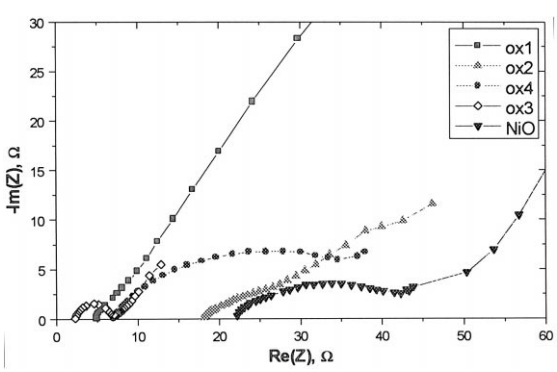

Fig. 5. Nyquist impedance diagram for the oxides in the frequency range of 10 mHz to 30 kHz. Time of immersion: 1 day.

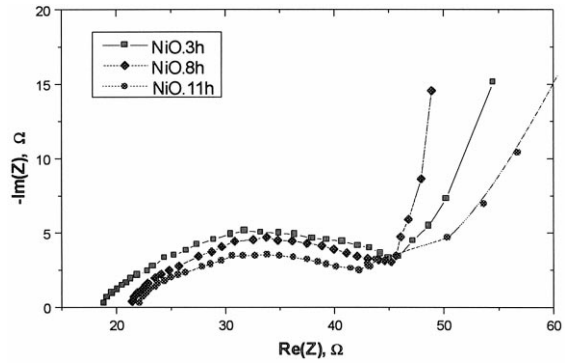

Fig. 6. Nyquist impedance diagram for NiO in the frequency range of 10 mHz to 30 kHz. Times of immersion: 3, 8 and 11 h.

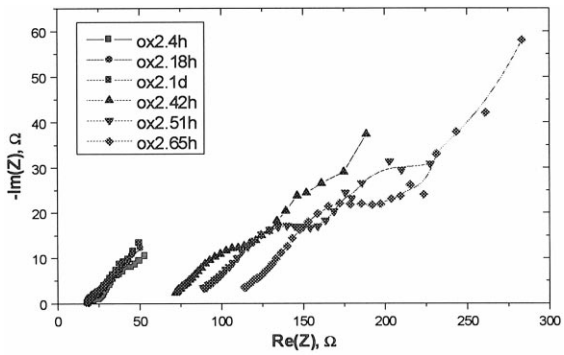

Fig. 8. Nyquist impedance diagram for oxide-2 in the frequency range of 10 mHz to 30 kHz. Times of immersion: 4, 18, 24, 42, 51 and 65 h.

homogeneous platelet-like grains (Fig. 4). The external layer thickness is about 50 μm and should correspond to the electrolyte penetration thickness. The external equiaxial grains could be the $LiCoO_2$-like grains and the platelet-like grains could correspond to the oxide-4-like structure. A lower porosity and a less reactive oxide can explain the high resistance of this latter material to the molten carbonate electrolyte.

In conclusion, the porosity, the degree of sintering and the composition of oxide play an important role in the material resistance to molten carbonate; the most resistant behaviour of the oxide-4, which contains Co and a lower Li content, could be explained by the higher values for each of these characteristics.

3.2. Electrochemical characterization

The EIS curves obtained after 1 day of immersion in molten carbonate show a different result for each oxide (Fig. 5). The NiO and the oxide-4 curves are similar with a deformed semicircular arc which corresponds to two partially superimposed semicircular arcs or to one semicircular arc in a non-homogeneous system. The semicircular arc of oxide-4 is bigger, thus, the charge transfer reaction is slower than for the NiO oxide. For the lower frequencies, the curve of these oxides also shows the beginning of another semicircular arc or line which may correspond to another electrochemical reaction or to a mass transfer phenomenon. The oxide-1 ($LiNiO_2$) curve is composed of two semicircular arcs (Figs. 5 and 7): a small and partly-obscured semicircular arc similar to the other oxides at higher frequencies and a large semicircular arc that is a little deformed. The diameter of this semicircular arc after 1 day of immersion is very prominent at about 500 Ω (Fig. 7), compared with the other oxides; only one portion is shown in Fig. 5. For the oxide-1, two charge transfer reactions have been detected, one very slow at lower frequencies and one fast at higher frequencies.

For the oxide-2, very deformed semicircular arcs are observed for the higher frequencies as for the oxide-4 and NiO but for low frequencies; the curve is not homogeneous because of the considerable dissolution suffered by this sample.

The oxide-3 shows a small semicircular arc at high frequencies and the beginning of another bigger semicircular arc or line for the lower frequencies.

In Fig. 6, it is apparent that the diameter of the semicircular arcs is decreasing with time and that the angle θ of the line observed at low frequencies with the x-axis is decreasing with time. This implies that, for the NiO oxide, the reaction rates are increasing slowly with time. In the case of the line at lower frequencies, it can be concluded

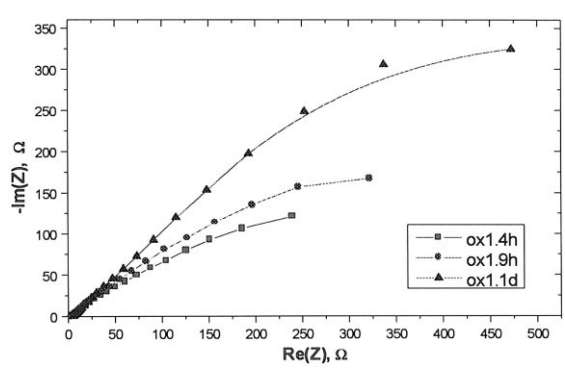

Fig. 7. Nyquist impedance diagram for oxide-1 in the frequency range of 10 mHz to 30 kHz. Times of immersion: 4, 9 and 24 h.

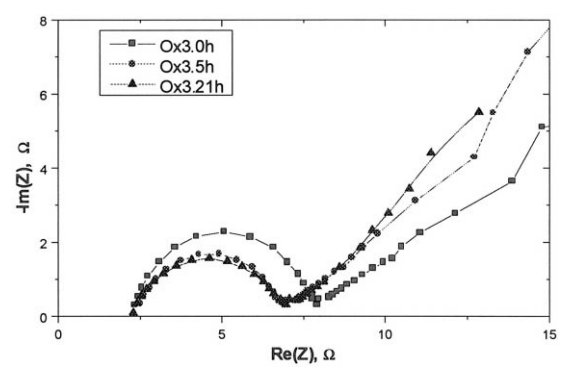

Fig. 9. Nyquist impedance diagram for oxide-3 in the frequency range of 10 mHz to 30 kHz. Times of immersion: 0, 5 and 21 h.

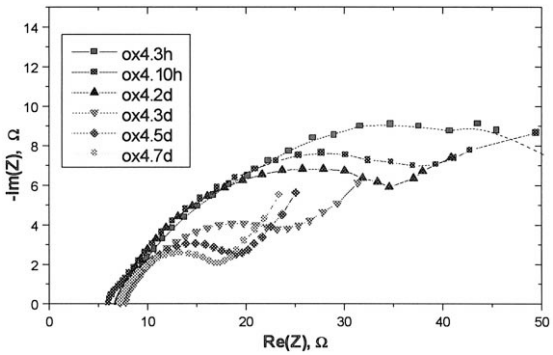

Fig. 10. Nyquist impedance diagram for oxide-4 in the frequency range of 10 mHz to 30 kHz. Times of immersion: 3, 10, 48, 72, 120 and 168 h.

that it does not correspond to a mass transport phenomenon because the angle θ differs from 45° or 90°. It is thought that this line does not correspond to a reaction of the oxygen reduction mechanism because it is not observed for all the oxides. It could correspond to a reaction of a metallic part (wire) of the electrode with the melt when the insulating ceramic becomes a little porous.

In the case of oxide-1 (Fig. 7), the semicircular arc at low frequencies increases with time suggesting that the corresponding reaction is decreasing rapidly with time. The higher diameter and the opposite variation with time of the observed semicircular arc, compared with the other oxides, could be due to an electrochemical reaction, different from the reactions observed for the other oxides.

For the oxide-2 (Fig. 8), significant dissolution in the electrolyte is shown by the shift of the curve on the *x*-axis with time. The shift begins after 1 day of immersion, the time necessary to change the electrolyte conductivity. This dissolution disturbs the system stability and thus the reliability of the data obtained.

In Fig. 9, it is shown that oxide-3 reaction rates are nearly constant after a few hours of immersion. A small increase of the second semicircular arc shows a small decrease in the second charge transfer reaction observed for this oxide.

The electrochemical reactions seem to accelerate with time at the oxide-4 interface as shown by the constant decrease of the semi-semicircular arc diameter between 3 h and 7 days in Fig. 10. Between 2 and 3 days, significant change of reaction rate occurred which can indicate a change in the structure of the cathode surface. After this change, a second semicircular arc or a line appears at the lower frequencies which had been observed during the first days by the high frequency semicircular arc.

4. Discussion

Two important phenomena need to be taken into account to analyze the results. The first is the evolution of the structure and the composition of the cathode material with time, as characterized by XRD and SEM. The second is the development of the electrochemical reactions which take place at the cathode–melt interface and which depend, in part, on the first phenomenon. EIS spectra show the development of the different electrochemical reactions at the cathode surface; thus, some hypothesis can be made about the variation of the cathode surface structure and properties.

The species which play a role in the electrochemical reactions in the gas–molten carbonate–cathode system under MCFC cathode conditions are O_2, CO_2 and H_2O. Indeed, it has been shown that water can have an important influence in the oxygen reduction mechanism in molten carbonate if the partial pressure of CO_2 is low, i.e., if the CO_2 concentration is lower than the O_2^- concentration in the melt [12].

The oxygen reduction mechanism under MCFC cathode conditions has been described as several elemental reactions [2–5] as follows:

$$O_2,CO_2(\text{gas}) \Leftrightarrow O_2,CO_2(\text{dissolved}) \quad (1)$$

$$O_2 + 2CO_3^{2-} \Leftrightarrow 2O_2^{2-} + 2CO_2 \quad (2)$$

$$O_2 + O_2^{2-} \Leftrightarrow 2O_2^- \quad (3)$$

$$O_2^- + e^- \Leftrightarrow O_2^{2-} \quad (\text{superoxide limiting reaction}) \quad (4)$$

$$O_2^{2-} + e^- \Leftrightarrow O^{2-} + (O^-) \quad (\text{peroxide limiting reaction}) \quad (5)$$

$$(O^-) + e^- \Leftrightarrow O^{2-} \quad (6)$$

$$O^{2-} + CO_2 \Leftrightarrow CO_3^{2-} \quad (7)$$

and is composed of two slower reactions (reactions (4) and (5)) that limit the oxygen reduction rate. These reactions are the reduction of the peroxide ions and the reduction of the superoxide ions. If the oxygen reduction mechanism is limited by a superoxide or a peroxide reduction reaction, then one semicircular arc should be observed on the EIS spectra; if it is limited by a mixed peroxide–superoxide reduction mechanism (with similar superoxide and peroxide reduction rates), there should be two semicircular arcs more or less superimposed.

The oxygen reduction mechanism can also be limited by CO_2 diffusion through the melt (reaction (7)) because of the low pressure of CO_2. In this case, a straight line should be observed at low frequencies on the EIS spectra.

In the case of the NiO oxide, it was possible to detect with the EIS technique the modification of the cathode structure through the decrease of the semicircular arc diameters. The fast NiO structure change facilitated by the initial porosity of the cathode. The higher porosity and the mixed oxide formation at the surface seems to increase the oxygen reduction rate.

In the case of the oxide-1 ($LiNiO_2$), the semicircular arc does not correspond to the oxygen reduction mechanism because of the excessive value of the semicircle diameter

(Fig. 7). It is thought that the arc corresponds to the reaction of a metallic part of cathode with the melt due to degradation of the insulating ceramic. Thus, it is impossible to find relationships between the EIS spectrum (Fig. 7) and the XRD and SEM characterizations in this case.

The EIS technique is very useful for detecting the dissolution (and its rate) of oxides in the melt but, when the dissolution is very fast, the curves obtained cannot give further information about the mechanism, as in the case of the oxide-2 (Fig. 8). The curves for longer times correspond to a virtual disappearance of the cathode, explaining their irregular shape.

The oxide-3 shows a result similar to the NiO oxide but the reduction kinetic seem a little faster and the variation of the reduction rate is lower (Fig. 9). As for the NiO oxide, there is no significant dissolution with time of the cathode. The better definition of the circle could be due to better preparation of the cathode and the second circle may be due to a reaction of a metallic part of the cathode with the melt. The uncertain behaviour detected by the XRD (Fig. 2) and SEM (Fig. 3) is not in accordance with the EIS result in this case. It can be explained by the fact that EIS curves corresponds to a shorter time of immersion than SEM and XRD results for practical reasons and that a change in the EIS curves may occur for longer times.

The oxide-4 shows a similar behaviour to NiO and oxide-3 but the variation of reaction rate is very noticeable with time. Indeed, at the beginning, the reduction rate of the peroxide–superoxide ions is relatively low compared with NiO and the oxide-3 but after 2 days, this rate begins to fall until it approaches the oxide-3 value. The more stable behaviour of oxide-4 after 3 days of immersion is also confirmed by the XRD and SEM which have shown the lower penetration of the melt into the matrix (Fig. 4) and transformation to another high lithium-content compound with time (Fig. 2).

5. Conclusions

From this work, we can conclude the following.

(1) The development of porosity and of the oxide present at the surface of the cathode has been shown to increase the oxygen reduction rate with time in the case of NiO, oxide-3 and oxide-4.

(2) The loss of electric contact for the electrode (oxide-1) or the marked dissolution of the sample (oxide-2) prohibit a satisfactory analysis of the mechanism or rate of reaction.

(3) The rate of peroxide or superoxide reduction is similar in the case of NiO, oxide-3 and oxide-4 but the well-formed semicircle obtained for the oxide-3 can be explained by the fact that only the superoxide or peroxide reaction occurs or that the electrical contact to the electrode was more secure than for NiO and oxide-4. In this hypothesis, we can say that only the superoxide or peroxide reaction is observed for these three oxides and that the vigour of the preparation influences the form of the semicircle.

(4) In this study, it was shown that the oxygen reduction mechanism was not limited by mass transport of CO_2 as in other studies [2–5] but by the charge transfer reaction of peroxide or superoxide reduction. It means that the CO_2 production by the system at the melt interface is sufficient to obtain a consequent CO_2 partial pressure at the surface of the melt and/or that the superoxide–peroxide reduction reactions are slower under these conditions.

(5) The oxide-3 allows the fastest oxygen reduction rate during the first day of immersion and the oxide-4 the fastest oxygen reduction rate for longer immersion times ($t > 3$ days) because of oxide-3 degradation (Fig. 2). The oxide-4 also suffers a transformation with time into a $LiCoO_2$-like structure but this is favorable to the reaction rate. The oxygen reduction rate in the presence of the NiO cathode is in between the value of the oxide-3 and the value of the oxide-4 during the first day of immersion that shows the well-behaved electrochemical properties of these two biphasic oxides.

(6) The oxide-4 shows the most stable behaviour in the long term immersion test despite a slight transformation of its surface structure. It seems that Co addition coupled with a lithium content lower than the metal content is the best option to improve the NiO properties.

(7) Longer term immersion tests are necessary to compare the dissolution rate of the oxides which exhibited the most stable behaviour (NiO, oxide-3 and oxide-4).

Acknowledgements

The authors wish to express their gratitude for financial support of this work to the Comunidad de Madrid (Project No. 07M/0521/1997).

References

[1] K. Tanimoto, M. Yanagida, T. Kojima, Y. Tamiya, H. Matsumoto, Y. Miyazaki, J. Power Sources 72 (1998) 77–82.
[2] I. Uchida, T. Nishina, Y. Mugikura, K. Itaya, J. Electroanal. Chem. 206 (1986) 229.
[3] C. Yuh, J.R. Selman, AIChE J. 34 (12) (1988) 1949.
[4] T. Nishina, I. Uchida, Proc. Symp. Molten Carbonate Fuel Cell Technol., The Electrochem. Soc. PV90 16 (1990) 438.
[5] T. Nishina, G. Lindbergh, T. Kudo, I. Uchida, The International Fuel Cell Conference Proceedings, NEDO (1992) 189–192.
[6] R.C. Makkus, PhD Thesis, Delf University of Technology, The Netherlands, 1991.
[7] R.C. Makkus, K. Hemmes, J.H.W. de Wit, J. Electrochem. Soc. 141 (12) (1994) 3429–3438.
[8] J.A. Prins-Jansen, G.A.J.M. Plevier, K. Hemmes, J.H.W. De Wit, Electrochim. Acta 41 (1996) 1323–1329.
[9] M. Azzi, J.J. Rameau, Corros. Sci. 30 (1990) 439.
[10] T. Nishina, S. Ohuchi, K. Yamada, I. Ichida, J. Electroanal. Chem. 408 (1996) 181–187.
[11] S. Freni, F. Barone, M. Puglisi, Int. J. Energy Res. 22 (1998) 17–31.

[12] S. Miyazaki, et al., Fuel Cell Seminar, San Diego, 1994, 120.
[13] L. Plomp, J.R. Veldhuis, E.F. Sitters, S.B. Van der Molen, J. Power Sources 39 (1992) 369–373.
[14] L. Giorgi, M. Crewska, M. Patriarca, S. Scaccia, E. Simonetti, A. Di Bartolomeo, J. Power Sources 49 (1994) 227–243.
[15] T.M.T.N. Tennakoon, J. Electrochem. Soc. 144 (1997) 2296–2301.
[16] T. Fukui, H. Okawa, T. Tsunooka, J. Power Sources 71 (1998) 239–243.
[17] B.Y. Yang, K.Y. Kim., in: D. Shores, H. Maru, I. Uchida, J.R. Selman (Eds.), Molten Carbonate Fuel Cell Technology, the Electrochemical Society Proceeding Series PV97-4, Pennington, NJ, 1997, pp. 286–295.
[18] K. Hatoh, J. Nikura, E. Yasumoto, T. Gamo, Denki Kagaku 64 (1996) 825–830.
[19] E. Antolini, L. Giorgi, Ceram. Int. 24 (1998) 117–124.
[20] J. Baranda, PhD Thesis, Universidad Autonoma de Madrid, Madrid, Spain, 1997.
[21] L. Daza, CSIC Report, Spain, December 1996.